ORIGINAL ARTICLE

Cancer Science WILEY

ZHX3 promotes the progression of urothelial carcinoma of the bladder via repressing of RGS2 and is a novel substrate of TRIM21

Minhua Deng[1,2] | Wensu Wei[1,2] | Jinling Duan[1] | Rixin Chen[1] | Ning Wang[1,2] | Leye He[3] | Yulu Peng[1,2] | Xiaodan Ma[1] | Zeshen Wu[1] | Jianye Liu[3] | Zhiyong Li[1,2] | Zhiling Zhang[1,2] | Lijuan Jiang[1,2] | Fangjian Zhou[1,2] | Dan Xie[1] 🆔

[1]State Key Laboratory of Oncology in South China, Collaborative Innovation Center for Cancer Medicine, Sun Yat-sen University Cancer Center, Guangzhou, China

[2]Department of Urology, Sun Yat-sen University Cancer Center, Guangzhou, China

[3]Department of Urology, Xiangya Third Hospital, Changsha, China

Correspondence
Fangjian Zhou and Dan Xie, State Key Laboratory of Oncology in South China, Collaborative Innovation Center for Cancer Medicine, Sun Yat-sen University Cancer Center, No. 651, Dongfeng Road East, Guangzhou 510060, China.
Emails: zhoufj@sysucc.org.cn (F.Z.); xiedan@sysucc.org.cn (D.X.)

Abstract

Clinically, patients with urothelial carcinoma of the bladder (UCB) with tumor metastasis are incurable. To find new therapeutic strategies, the mechanisms underlying UCB invasion and metastasis should be further investigated. In this study, zinc finger and homeobox 3 (ZHX3) was first screened as a critical oncogenic factor associated with poor prognosis in a UCB dataset from The Cancer Genome Atlas (TCGA). These results were also confirmed in a large cohort of clinical UCB clinical samples. Next, we found that ZHX3 could promote the migration and invasion capacities of UCB cells both in vitro and in vivo. Mechanistically, coimmunoprecipitation (coIP) and mass spectrometry (MS) analysis indicated that ZHX3 was a target of tripartite motif 21 (TRIM21), which mediates its ubiquitination, and subsequent degradation. Notably, RNA-seq analysis showed that ZHX3 repressed the expression of regulator of G protein signaling 2 (RGS2). Generally, our results suggest that ZHX3 plays an oncogenic role in UCB pathogenesis and might serve as a novel therapeutic target for UCB.

KEYWORDS
regulator of G protein signaling 2, transcription repression factor, tripartite motif 21, urothelial carcinoma of the bladder, zinc finger and homeobox 3

1 | INTRODUCTION

UCB is one of the most common and lethal malignancies among urinary cancers and is markedly heterogeneous.[1,2] Even if RC is performed, half of patients with MIBC eventually experience relapse or metastasis. Clinically, most UCB-related deaths are associated with cancer metastasis. Therefore, a deeper study of the potential molecular mechanisms involved in UCB is urgently needed to develop more efficient anticancer treatments.

In cancers, gene amplification is a universal phenomenon and may be related to the development of cancers. *AIB1*,[3] *ZNF217*, *BTAK*, and *PTPTN1*[4-6] are all located in 20q, a region that includes some candidate oncogenes. Similarly, our previous report demonstrated that amplification of the long arm of chromosome 20 was frequently detected in human UCB.[7] By screening the UCB dataset from TCGA, we identified that zinc finger and homeobox 3 (*ZHX3*) was either gained or amplified in 59.6% (243/408) of patients with UCB. The *ZHX3* gene, which is mapped to chromosome 20q12, has been found to be associated with many kinds of biological processes, such as cell differentiation and metabolism.[8,9] It has been suggested that ZHX3 is a ubiquitous transcriptional repressor expressed in human cells and tissues.[10] Recently, a growing number of studies have revealed that the ZHX protein is associated with various cancers, including breast cancer, renal cancer, and cholangiocarcinoma.[11-13] However, the potential function of ZHX3 in UCB pathogenesis and its clinical and/or survival significance in UCB are still unclear.

In this study, we identified for the first time that *ZHX3* is a potential oncogenic factor in UCB pathogenesis and verified the biological function of ZHX3 in UCB through in vivo and in vitro experiments. Further mechanistic study explored the potential signaling pathway of ZHX3 in UCB pathogenesis. Overall, our study highlights that ZHX3 is a potential therapeutic target for UCB.

2 | MATERIALS AND METHODS

2.1 | Cell lines and cell cultures

Seven cell lines, including 293T, TCC-SUP, T24, 5637, RT4, UMUC-3, and SV-HUC-1, were used in our study. All cell lines were obtained from the ATCC. T24 and 5637 cells were cultured in RPMI 1640 medium (Invitrogen, Carlsbad, CA, USA) supplemented with 10% fetal bovine serum (HyClone) and 1% antibiotics. 293T, TCC-SUP, UMUC-3, RT4, and SV-HUC-1 cells were cultured in DMEM (Invitrogen) supplemented with 10% fetal bovine serum (H Clone) and 1% antibiotics. All cells were grown in a humidified incubator at 37°C with 5% CO_2 in air.

2.2 | RNA interference (RNAi)

The short interfering RNAs (siRNA) for knockdown of TRIM21 and RGS2 were obtained from RIBOBIO (GuangZhou). The short hairpin RNAs (shRNAs) for knockdown of ZHX3 and RGS2 were purchased from GeneCopeia. The target sequences for siRNAs and shRNAs are recorded in Table S1.

2.3 | Plasmid construction and retroviral infection

The ZHX3 overexpression plasmid was obtained from Furuibio (Guangzhou). The Myc-TRIM21 overexpression plasmid and the wild-type human RGS2 promoter cloned into the pGL3-Basic luciferase reporter plasmid were obtained from GeneCreate.

The relevant UCB cell lines were transfected with Lipofectamine 3000 reagent (Invitrogen) in accordance with the manufacturer's instructions. For selected stable UCB cell lines, 0.5-1.0 µg/mL puromycin or/and 50-100 µg/ml Geneticin was for used several days.

2.4 | Patients and specimen characteristics

In our study, the paraffin sections used for immunohistochemistry (IHC) were obtained from patients who underwent RC between February 2000 and February 2014 at Sun Yat-sen University Cancer Center (Guangzhou, China). None of the patients had distant metastasis before surgery, and postoperative pathology results confirmed that the paraffin sections of all patients were urothelial carcinoma, cases with carcinoma in situ confirmed by pathology were excluded from our study. The TNM staging method is based on the eighth edition of the Union International Contre le Cancer (UICC, 2017)[14]. Before the study, all patients signed an informed consent form. The human UCB tissues used in this study were approved by the medical ethics committee of Sun Yat-sen University Cancer Center.

2.5 | Immunohistochemistry

The method used for the IHC study was performed as previously reported.[15]

The staining index was recorded as negative = 0, weak = 1, moderate = 2, or strong = 3. The percentage of positively stained areas was scored as follows: <10%, 1; 10%-40%, 2; 40%-70%, 3; >70%, 4. The final IS was the product of the staining index and the positive area score (0-4, low expression; 6-12, high expression). Two independent pathologists who were blinded to the patient's clinical parameters separately assessed the IS. The anti-ZHX3 (SAB1402549, 1:200 dilution; Sigma-Aldrich) and anti-RGS2 (PA528162, 1:200 dilution; Invitrogen) antibodies were used for IHC.

2.6 | Western blotting assay

First, lysates containing the same amount of protein mixed with 1× SDS were resolved by SDS-PAGE and transferred to PVDF membranes (Millipore). Second, the membranes cut into suitable sizes

were incubated with the corresponding antibodies at 4°C overnight. Third, the membranes were incubated with the secondary antibody at room temperature for 1 h. Finally, immunoreactivity was detected using the Enhanced Chemiluminescence kit (Amersham Biosciences). Antibodies used in the western blot analysis are listed in Table S2.

2.7 | Quantitative real-time polymerase chain reaction

TRIzol reagent (Invitrogen) was used to extract total RNA from UCB cells. In accordance with the manufacturer's protocol of the PrimeScript RT reagent kit (TaKaRa), 1 μg of total RNA was reverse transcribed to generate cDNA. The quantitative real-time PCRs were completed using SYBR Green SuperMix (Roche). The corresponding primer sequences are displayed in Table S3.

2.8 | Transwell assays

In total, 5×10^4 sh-ZHX3 and sh-NC UCB cells or 3×10^4 T24-Vector and T24-ZHX3 UCB cells were placed into the inside of the chamber with Matrigel-coated Boyden invasion chambers (BD Biosciences) in 200 μL of serum-free RPMI 1640 medium, then 600 μL of RPMI 1640 medium containing 10% FBS were added to the outside of the chamber, which was placed in a 24-well plate. After incubation for 24 h at 37°C, the outside membrane was transferred to a new 24-well plate with 4% paraformaldehyde and stained in crystal violet (Sigma). All experiments were performed 3 times.

2.9 | Wound-healing assays

UCB cells were spread in 6-well plates and grown to 100% density. A sterile 10-μl pipette tip was used to scratch each well. Then, the floating cells were washed away with PBS, and the adherent cells were cultured in serum-free medium. Changes in the scratches were recorded under an inverted microscope (Nikon Eclipse 80i) at 0 and 24 h. All experiments were performed 3 times.

2.10 | Coimmunoprecipitation, silver staining, and mass spectrometry

Coimmunoprecipitation (coIP) was performed in accordance with a previous method.[16] Only proteins detected by ZHX3 Flag and unique peptides > 0 were considered to be significantly differentially expressed.

2.11 | Dual-luciferase reporter assay

The RGS2-promoter fragment was cloned into the pGL3 plasmid with a luciferase reporter gene. Then, T24 cells

with or without overexpression of ZHX3 were spread onto a 6-well plate and cultured until they reached 50% density. We used Lipofectamine 3000 to cotransfect the reporter plasmid and pRL-TK Renilla luciferase plasmid into T24 cells. Finally, we detected the luciferase activity of firefly and Renilla with the Dual-Luciferase Reporter System Kit (E1910; Promega).

2.12 | Animal models

All animal experiments in this study were approved by the animal ethics committee at our institution. Four-wk-old BALB/c nude mice were obtained from GemPharmatech. Then, 1×10^6 T24 cells were injected via the tail vein for each mouse. At 6 wk later, the mice were sacrificed to assess tumor growth. The IVIS 200 imaging system was used to observe changes in the tumor.

2.13 | Other methods

The methods for immunofluorescence, ubiquitination assay, and active Rho detection assay are included in Supplementary Materials and Methods.

2.14 | Statistical analysis

Every experiment was performed at least 3 times, and the data are presented as the mean value ± standard deviation. Appropriate statistical methods were used in this study, including the chi-square test, Fisher exact test, Student two-tailed *t* test, the log-rank test, and Cox regression analysis. When the *P*-value was < .05, the results were considered statistically significant.

3 | RESULTS

3.1 | ZHX3 frequently exhibits gain or amplification in UCB and is positively correlated with worse clinical parameters in patients with UCB

In this study, by analyzing data from 408 patients with UCB from the TCGA database, we found that *ZHX3* was gained or amplified in 59.6% (243/408) of patients with UCB (Figure 1A). The gain or amplification of *ZHX3* copy number was positively correlated with the high expression levels of ZHX3 mRNA (Figure 1B). In advanced stage and high-grade bladder cancer, the copy number of the *ZHX3* gene in more than 50% of cases was gain or amplification (Figure 1C, D). This means that there was a positive trend between ZHX3 copy number changes and advanced bladder cancer. In
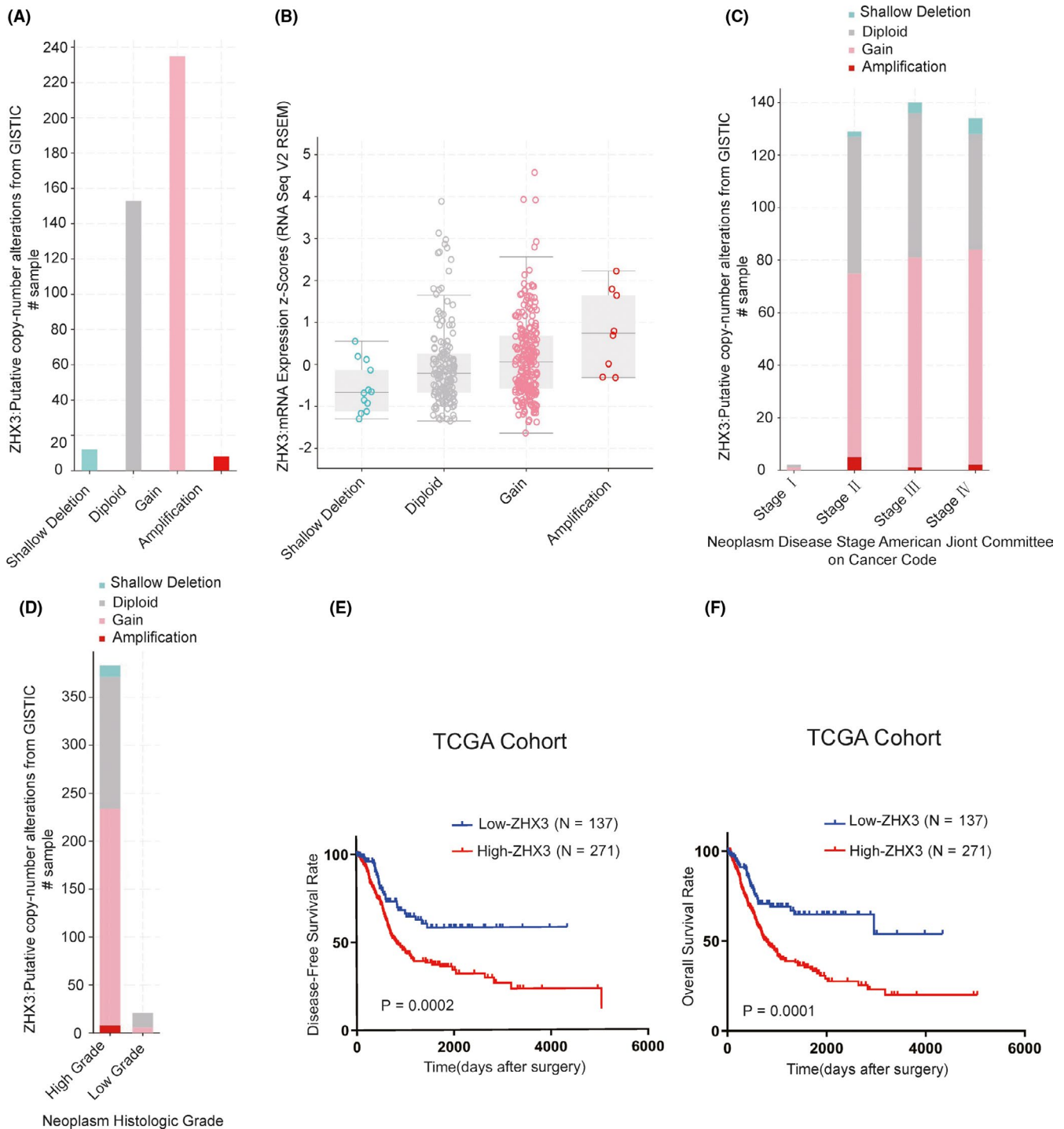
FIGURE 1 ZHX3 has been identified as an oncogenic factor in UCB and is associated with poor DFS and OS in patients with UCB. A, The *ZHX3* gene either showed gain or amplification in patients with UCB from the TCGA database. B, Gain or amplification of *ZHX3* was positively correlated with the high level of *ZHX3* mRNA expression. C, D, The copy number of *ZHX3* was positively correlated with worse clinical parameters. E, F, Prognostic significance of ZHX3 in 408 patients with UCB assessed by Kaplan-Meier analysis

addition, the results showed that high ZHX3 expression was associated with shorter DFS and OS in 408 patients with UCB with *ZHX3* gene expression data from the TCGA database through Kaplan-Meier analyses (Figure 1E,F). These results indicated that *ZHX3*, located in 20q12, is a gene with potential oncogene function in the progression of UCB.

3.2 | ZHX3 is always upregulated in patients with UCB and can be regarded as an independent prognostic factor in UCB

To confirm the results drawn from the TCGA database cohort, we detected the ZHX3 protein expression levels in 199 UCB

tissues and 10 paired non-neoplastic bladder tissues from patients who underwent RC at Sun Yat-sen University Cancer Center in Guangzhou, China. The IHC results showed that ZHX3 was highly expressed in tumor cell nuclei in 105/199 UCB samples, whereas non-neoplastic bladder tissues had inadequate or low levels of ZHX3 in the nucleus. IHC staining of ZHX3 in typical cases of UCB and non-neoplastic bladder tissues is shown in Figure 2A. Correlation analysis showed that high ZHX3 expression was positively correlated with worse clinical parameters, including advanced T stage, N stage, and recurrence status (Table 1). Kaplan-Meier analysis confirmed that patients with UCB with high ZHX3 expression had poorer DFS ($P < .001$; Figure 2B) and shorter OS ($P < .001$, Figure 2C). Furthermore, multivariate Cox regression analysis found that high ZHX3 expression could be an independent factor, suggesting adverse prognosis in patients with UCB (Table 2).

3.3 | Characterization of ZHX3 protein expression in UCB tissues and cells

To investigate ZHX3 expression in UCB tissues, we collected 12 pairs of fresh primary UCB tissues and adjacent non-neoplastic tissues from patients at our center. The results showed that ZHX3 was highly expressed in 9/12 of UCB tissues compared with paired adjacent non-neoplastic tissues (Figure 3A). Five cancer cell lines showed clearly upregulated endogenous expression of ZHX3 compared with the normal uroepithelial cell line SV-HUC-1 as examined by western blotting (Figure 3B). These results suggested that the upregulated expression of ZHX3 protein may be a tumor-specific event.

3.4 | ZHX3 promotes UCB cell migration and invasion capacities in vitro and in vivo

Next, we evaluated the biological roles of ZHX3 in UCB. Based on their endogenous ZHX3 expression levels, T24 and UMUC-3 cells were selected to create 2 cell lines with stable ZHX3 knockdown, and T24 cells were also used to construct a ZHX3 overexpression cell line. The results showed that knockdown of ZHX3 using 2 shRNAs resulted in decreased ZHX3 protein levels (Figure 3C). Transwell and wound-healing assays demonstrated that silencing ZHX3 markedly suppressed both the capacities of migration and invasion in T24 and UMUC-3 cells. Conversely, exogenously increased ZHX3 expression in T24 cells significantly increased cell migration and invasion activities (Figure 3D, E). However, knocking out ZHX3 in SV-HUC-1 cells did not affect the cell migration and invasion activities (Figure S1).

Subsequently, to validate the function of ZHX3 in UCB metastasis in vivo, T24 cells with or without knockdown of ZHX3 were injected into 4-wk-old BALB/c nude mice separately via the tail vein. Six wk later, the mice were put to death, and the lung metastatic nodules were examined. The results demonstrated that the mice injected with ZHX3-knockdown cells had markedly fewer lung metastatic nodules compared with mice injected with control T24 cells (Figure 3F). Meanwhile, the results of the bioluminescent imaging were also validated by general images and H&E staining of the lung metastatic nodules (Figure 3G).

3.5 | ZHX3 expression levels were downregulated by TRIM21 through ubiquitination and degradation

To further explore the potential mechanisms by which ZHX3 promotes UCB cell metastasis, we used whole-cell lysates from

(A)

Non-tumor   Tumor-case 1   Tumor-case 2

(B) Low-ZHX3 (N = 94) / High-ZHX3 (N = 105)
Disease-Free Survival Rate
P = 0.0001
Time(months after surgery)

(C) Low-ZHX3 (N = 94) / High-ZHX3 (N = 105)
Overall Survival Rate
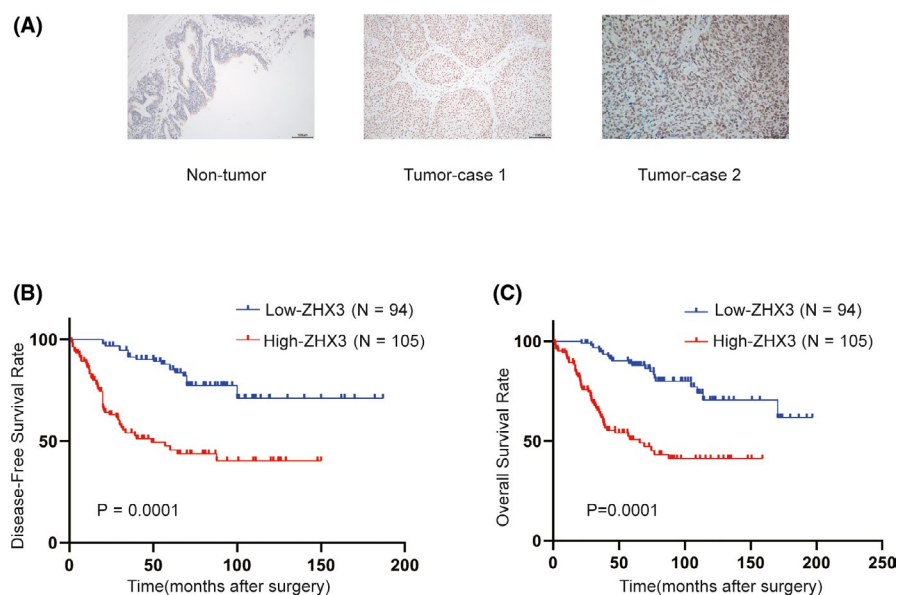P=0.0001
Time(months after surgery)

FIGURE 2 ZHX3 is highly expressed in UCB tissues and predicts worse patient survival in UCB. A, Representative images of IHC staining for ZHX3 in non-neoplastic bladder and bladder cancer tissues. B, C, High expression levels of ZHX3 were correlated with poor DFS and OS in patients with UCB

TABLE 1 Correlation expression of ZHX3 and clinicopathological variables in 199 cases of patients with UCB in SYSUCC

| Variable | All cases (N = 199) | ZHX3 expression (%) | | P value[a] |
		Normal expression (N = 94)	Overexpression (N = 105)	
Age (years)				
≤60	102	50 (49.0)	52 (51.0)	.605
>60	97	44 (45.4)	53 (54.6)	
Gender				
Female	21	12 (57.1)	9 (42.9)	.336
Male	178	82 (46.1)	96 (53.9)	
Smoking history				
No	92	44 (47.8)	48 (52.2)	.877
Yes	107	50 (46.7)	57 (53.3)	
PT status				
T1	46	28 (60.9)	18 (39.1)	.035
T2-T4	153	66 (43.1)	87 (56.9)	
pN status				
pN-	158	81 (51.3)	77 (48.7)	.025
pN+	41	13 (31.7)	28 (68.3)	
Histological grade (WHO, 2004)[38]				
Low grade	71	39 (54.9)	32 (45.1)	.105
High grade	128	55 (43.0)	73 (57.0)	
Recurrence				
No	112	72 (64.3)	40 (35.7)	.001
Yes	87	22 (25.3)	65 (74.7)	

Abbreviations: UCB, Urothelial carcinoma of the bladder.
[a]Chi-square test.

T24-ZHX3-Flag and T24-Vector-Flag cells to conduct immunoprecipitation experiments. The protein bands in the resultant immunoprecipitates were detected by silver staining (Figure 4A). Next, MS was used to identify the proteins pulled down, and the results showed that TRIM21 exhibited a high degree of interaction with the ZHX3 protein (The top 10 proteins that bound to ZHX3-Flag in further MS analysis are listed in Table S4). The interaction between TRIM21 and ZHX3 was confirmed by coIP in T24 cells (Figure 4B), and colocalization of TRIM21 and ZHX3 in UCB cells was confirmed by immunofluorescent staining (Figure 4C).

Considering that TRIM21 has been regarded as an E3 ubiquitin ligase,[17] we hypothesized that ZHX3 was regulated by TRIM21 through proteasomal degradation. Upon initial investigation, we found that knockdown of TRIM21 markedly increased the ZHX3 protein levels, and overexpression of TRIM21 decreased the ZHX3 protein levels in T24 cells. However, there was no obvious change in TRIM21 protein levels after knockdown of ZHX3 in T24 cells (Figure 4D). No obvious correlation was observed between ZHX3 and TRIM21 mRNA levels (Figure 4E). Furthermore, after cycloheximide (CHX) was added to the cell culture medium, overexpression of TRIM21 could accelerate the degradation of the ZHX3 protein (Figure 4F). Based on these results, we believe that ZHX3 is regulated by TRIM21 through posttranscriptional regulation. Next, we performed a ubiquitination assay by cotransfecting si-NC or si-TRIM21 with or without HA-ubiquitin in T24 Flag-ZHX3, and then cultured with MG132 for 8 h. The results showed that the amount of ubiquitination of Flag-ZHX3 was low in cells with knockdown of TRIM21. In contrast, overexpression of TRIM21 significantly increased the levels of polyubiquitinated Flag-ZHX3 (Figure 4G, H). These data suggest that ZHX3 is a downstream target gene of TRIM21 that regulates the stability of the ZHX3 protein.

3.6 | ZHX3 represses RGS2 expression in UCB cells

Given that ZHX3 has been shown to act as a transcriptional repression factor[18] and to promote the capacities of migration and invasion in UCB cells, we wondered whether ZHX3 can repress certain unknown genes in the pathogenic process of UCB. The differential mRNA expression patterns of T24-shZHX3 and T24-shNC cells were compared with a PCR array of 84 metastasis-related genes. Four upregulated genes (*BMP2*, *MMP3*, *RGS2*, and *FGFBP1*) and 1 downregulated gene (*CDH2*) were identified because of a more than a 2-fold change in mRNA levels in T24-shZHX3 cells (Figure 5A). Changes in the mRNA expression levels were subsequently confirmed by protein detection. The results showed that *RGS2* and *CDH2* were validated as potential target genes of ZHX3 by western blot analysis (Figure 5B). A previous study demonstrated that epigenetic repression of RGS2 could promote bladder cancer progression[19], therefore we assume that *RGS2* is a downstream target of ZHX3. To confirm this relationship, we detected the expression of ZHX3 and RGS2 at the mRNA and protein levels. The results showed that when ZHX3 was knocked down in UCB cells, RGS2 was upregulated. In contrast, overexpression of ZHX3 resulted in reduced levels of RGS2 in UCB cells (Figure 5C,D).

As ZHX3 has previously been reported to act as a transcriptional repressor,[10] we investigated whether RGS2 was downregulated by ZHX3 through the same mechanism. The promoter region of RGS2 was cloned into the pGL3-basic plasmid with a luciferase reporter gene and cotransfected with the pRL-TK plasmid into T24-ZHX3 or T24-Vector UCB cells. An approximately 2-fold increase in luciferase activity in T24-Vector cells was observed in comparison with that in T24-ZHX3 cells, whereas in shZHX3 cells, the luciferase activity was more than 2-fold that in sh-NC cells (Figure 5E). These results indicated that RGS2 is the target gene repressed by ZHX3.

3.7 | Knockdown of RGS2 restores the migration and invasion capacities of UCB cells with ZHX3 knockdown

To further study the functional correlation between ZHX3 and RGS2, rescue experiments were performed. RNA interference was used to deplete RGS2 expression in ZHX3-knockdown T24 cells.

Variable	All cases	Univariate analysis[a] HR (95% CI)	P-value	Multivariate analysis[b] HR (95% CI)	P-value
Age (years)					
≤60	102	1.0	.038	1.0	.029
>60	97	1.657 (1.027-2.674)		1.727 (1.058-2.818)	
Gender					
Female	21	1	.174		
Male	178	1.699 (0.796-3.624)			
Smoking history					
No	92	1	.834		
Yes	107	1.052 (0.654-1.692)			
pT status					
T1	46	1	.001	1.0	
T2-T4	153	3.499 (1.599-7.656)		2.338 (1.029-5.312)	.043
pN status					
pN-	158	1	.001	1.0	.001
pN+	41	3.566 (2.086-6.098)		2.541 (1.435-4.501)	
Histological grade (WHO, 2004)[38]					
Low grade	71	1	.001	1	.032
High grade	128	3.044 (1.687-5.493)		1.995 (1.060-3.757)	
ZHX3					
Normal expression	94	1	.001	1.0	.001
Overexpression	105	4.029 (2.361-6.878)		2.749 (1.529-4.941)	
Recurrence					
No	112	1	.001	1	.021
Yes	87	2.851 (1.722-4.720)		1.914 (1.102-3.323)	

Abbreviations: CI, confidence interval; HR, hazards ratio; UCB, Urothelial carcinoma of the bladder.

[a]Univariate Cox regression model.

[b]Multivariate Cox regression model.

The results of the transwell and wound-healing assays revealed that RGS2 knockdown markedly restored the migration and invasion capacities of ZHX3-knockdown cells (Figure 6A,B). In our in vivo mouse model, we obtained similar results. The decreased number of metastatic nodules in the lungs of mice injected with ZHX3-knockdown UCB cells was largely restored in mice injected with the same cells with RGS2 knockdown (Figure 6C,D). These results suggested that ZHX3 promotes UCB cell invasion and migration by regulating RGS2.

3.8 | ZHX3 could activate RhoA by repressing RGS2

Previous studies indicated that RGS2 could inhibit the G protein signaling pathway by interacting with Gα subunits of the G protein and accelerating GTPase activity.[20] Furthermore, Gα subunits can affect the activity of RhoA by binding to and activating some RhoGEFs.[21] Therefore, we wondered whether ZHX3 impacts RhoA activity through RGS2 in UCB cells. The relationship between total RhoA and ZHX3 was investigated by western blot analysis. We found that, after knocking down ZHX3, RhoA expression was decreased in UCB cells. However, knocking down RGS2 restored the level of RhoA expression in sh-ZHX3 cells (Figure 6E). Next, we examined the levels of GTP-bound RhoA by using a pull-down assay. The results showed that RhoA activity was decreased in ZHX3-knockdown cells compared with ZHX3-control cells, but was significantly increased in ZHX3-knockdown UCB cells subjected to siRGS2 (Figure 6F). These results indicated that ZHX3 promotes UCB cell aggressiveness through the RGS2-RhoA pathway.

3.9 | Clinical significance of ZHX3 and RGS2 in human patients with UCB

Finally, we validated the clinical significance of ZHX3 and RGS2 in human patients with UCB. The expression of ZHX3 was negatively correlated with RGS2 in our cohort of UCB tissues (Figure 7A, P= .022). Further Kaplan-Meier analysis revealed that patients with

FIGURE 3 The levels of ZHX3 expression were consistent with the tumorigenic activity of UCB cells. A, ZHX3 expression in 12 pairs of UCB tissues. N, non-neoplastic bladder tissues; T, tumor tissue. Gapdh was used as a loading control. B, Expression levels of ZHX3 in five human UCB cell lines (ie, TCC-SUP, T24, UM-UC-3, BIU, RT4, and 5637) and 1 normal uroepithelial cell line, SV-HUC-1. Gapdh was used as a loading control. C, ZHX3 was efficiently knocked down or overexpressed in the corresponding cells by western blotting. D, Transwell assays show that the invasive capacity of UCB cells was inhibited when ZHX3 was knocked down. However, overexpression of ZHX3 cells had a higher invasive capacity compared with T24-Vector cells. Error bars indicate the means ± standard deviation (SD) of 3 independent experiments. **$P < .01$. E, Wound-healing assays show that the migration capacity of UCB cells was inhibited when ZHX3 was silenced. F, Silencing ZHX3 inhibited the metastatic ability of T24 cells in mouse models (6 mice per group). Bioluminescence imaging was performed at 0 and 6 wk after injection for each mouse. Representative bioluminescent images are shown. The mean bioluminescent signals are shown in the column. Error bars indicate the mean ± SD. ns: negative significance, **$P < .01$. G, Representative lung metastatic nodules (indicated by arrows) and H&E staining of lung tissue are shown (original magnification: ×100; scale bar: 100 μm). Lung tissue was taken from the mice at 6 wk after injection of UCB cells. ns: negative significance. **$P < .01$. Error bars indicate the mean ± SD
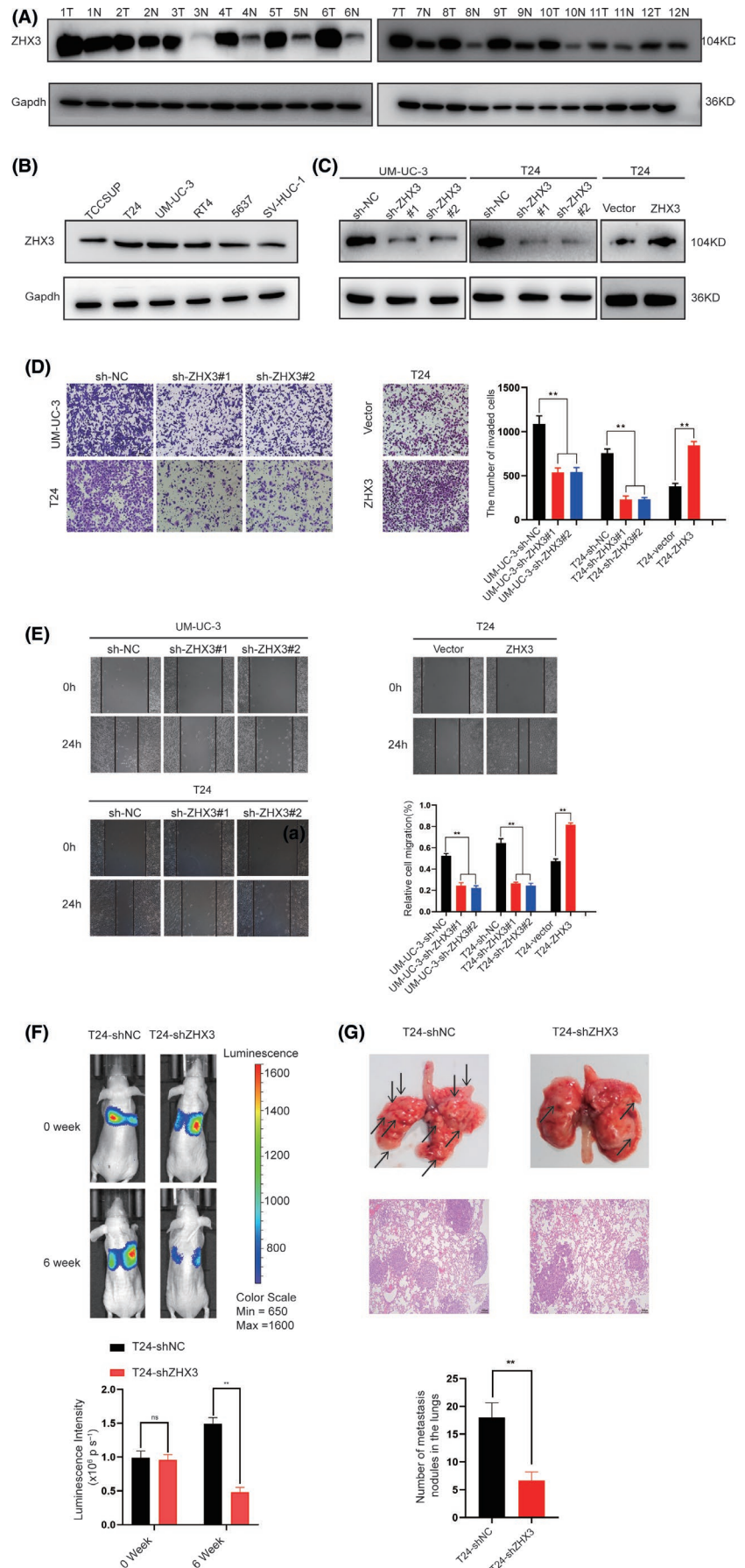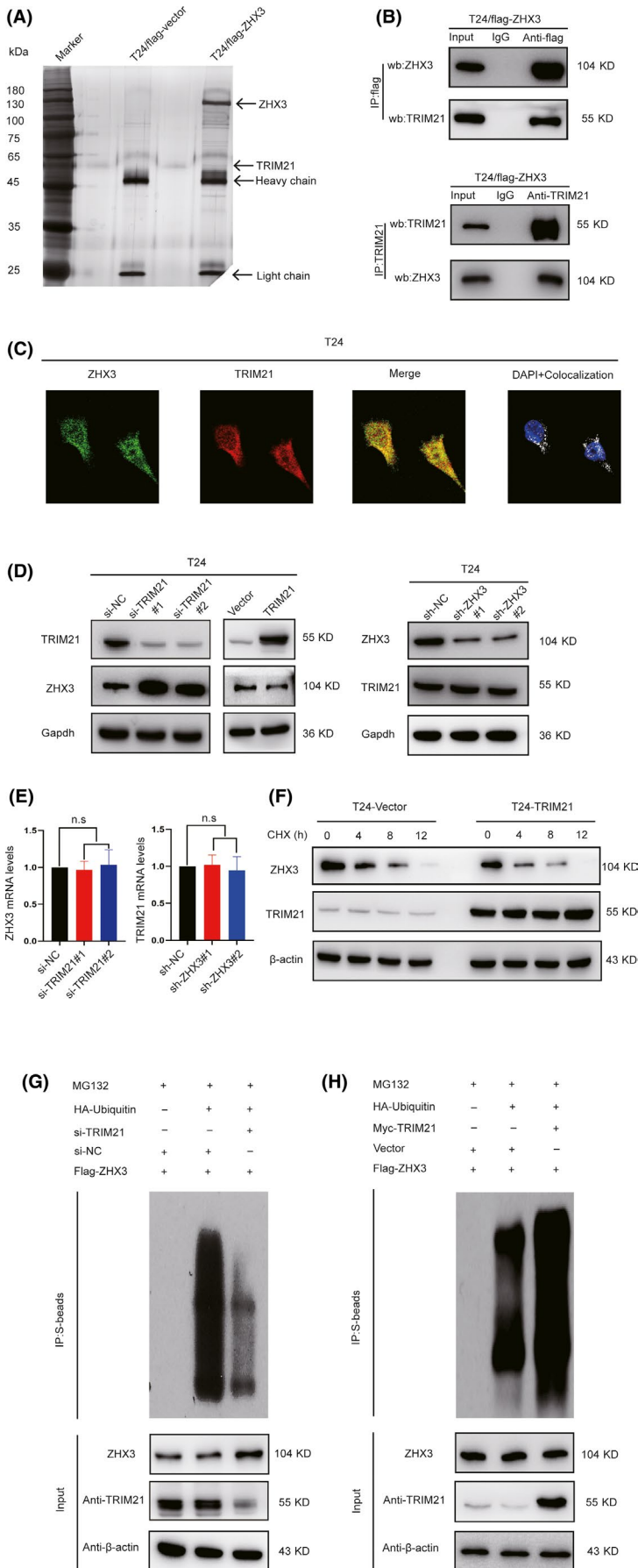
FIGURE 4 TRIM21 downregulates ZHX3 expression in UCB cell ubiquitin-mediated degradation. A, Silver staining results showed the protein bands that bind to ZHX3, and mass spectrometry was used to identify these proteins. The band corresponding to TRIM21 is indicated by an arrow. B, CoIP results show the relationship between TRIM21 and ZHX3 in T24 cells with stable ZHX3 overexpression. C, Confocal staining revealed the colocalization of TRIM21 and ZHX3 in T24 cells. D, Knockdown and overexpression of TRIM21 resulted in increased or decreased ZHX3 protein levels, although TRIM21 protein levels had no obvious change after knockdown of ZHX3. E, Silencing TRIM21 by siRNA in T24 cells resulted in no obvious change in ZHX3 mRNA levels. Similarly, there was no obvious change in TRIM21 mRNA levels in ZHX3-silenced shRNA in T24 cells. Error bars indicate the means ± SD of 3 independent experiments. ns: negative significance. F, The T24-Vector and T24-TRIM21 cells were cultured and treated with 50 µg/mL CHX. Cells were harvested at 0, 4, 8, or 12 h, and the levels of ZHX3 protein were detected by western blotting. G, In T24-Flag-ZHX3 cells, si-NC, or si-TRIM21 cotransfected with or without HA-ubiquitin plasmids. Before harvest, cells were cultured with 10 µM MG132 for 8 h. Cell lysates were immunoprecipitated with Flag antibody and immunoblotted as indicated. H, In T24-Flag-ZHX3 cells, Vector, or Myc-TRIM21 plasmids cotransfected with or without HA-ubiquitin plasmids. Before harvest, cells were cultured with 10 µM MG132 for 8 h. Cell lysates were immunoprecipitated with Flag antibody and immunoblotted as indicated

FIGURE 5 ZHX3 binds to the RGS2 promoter and represses RGS2. A, The 5 genes BMP2, MMP3, RGS2, FGFBP1, and CDH2 showed >2-fold change in mRNA expression in T24-shZHX3 cells compared with that in T24-shNC cells based on the Human Tumor Metastasis RT2 Profiler PCR Array. B, Analysis of the protein levels of BMP2, MMP3, RGS2, FGFBP1, and CDH2 by western blotting. C, Changes in RGS2 mRNA levels after ZHX3 knockdown or overexpression. Silencing ZHX3 with shRNA in T24 cells resulted in substantially increased *RGS2* mRNA levels, but overexpressing ZHX3 resulted in reduced mRNA levels of *RGS2*. The columns represent the means ± SD of 3 independent experiments. D, Changes in RGS2 protein levels after ZHX3 knockdown or overexpression. Silencing ZHX3 with shRNA in T24 cells resulted in substantially increased RGS2 protein levels, but overexpressing ZHX3 resulted in reduced protein expression of RGS2. E, ZHX3 represses RGS2 promoter activity. The pGL3 plasmid with the RGS2 promoter region and pRL-TK plasmid were cotransfected into T24-shNC, T24-shZHX3, T24-Vector, and T24-ZHX3 cells, which were subjected to a dual-luciferase activity assay. Cells overexpressing ZHX3 showed inhibited RGS2 promoter activity, however RGS2 promoter activity was increased when *ZHX3* was knocked down in T24 cells. The columns represent the means ± SD of 3 independent experiments. **$P < .01$
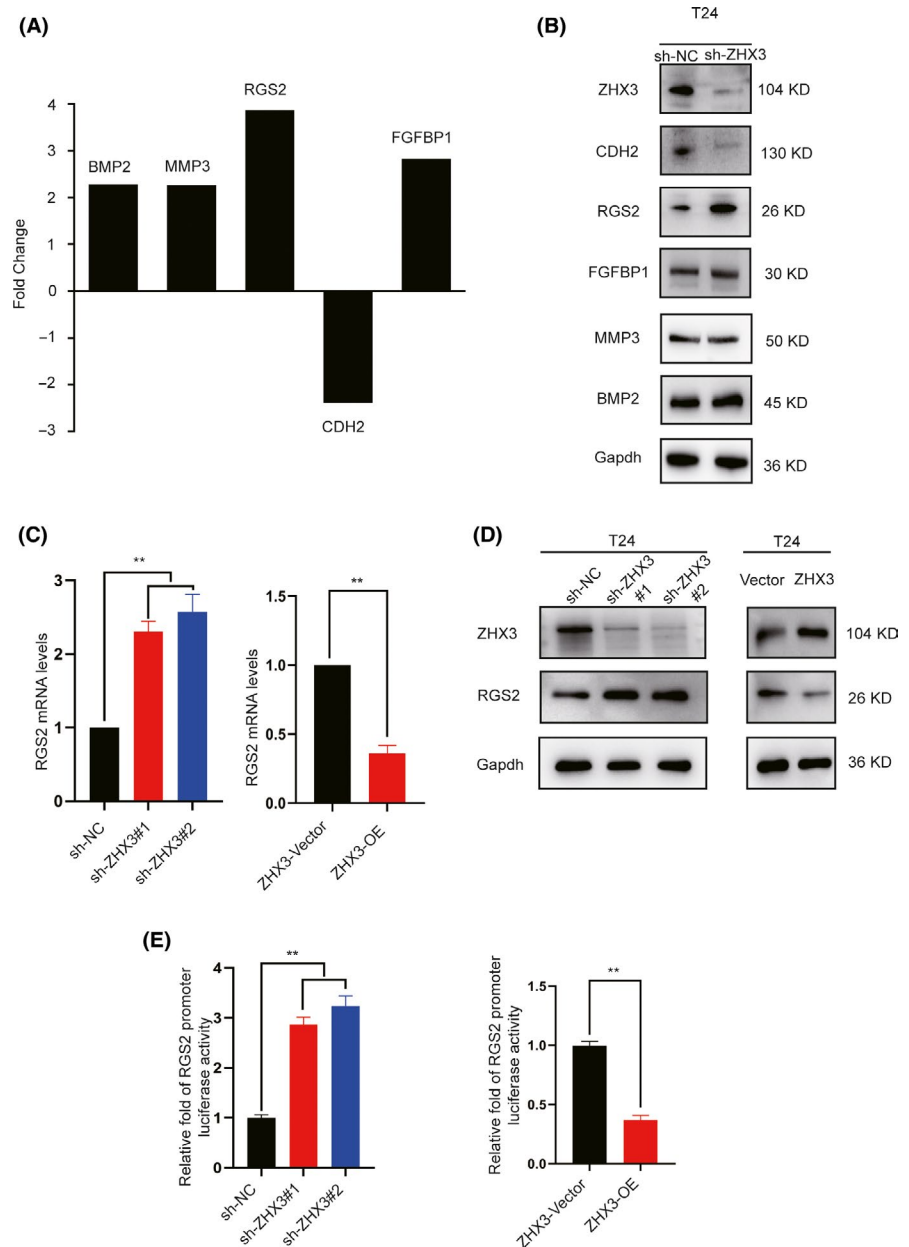
both low ZHX3 and high RGS2 expression had the best survival rate. However, patients with high ZHX3 and low RGS2 expression had the worst prognosis. (Figure 7B,C).

4 | DISCUSSION

In patients with UCB, metastasis is incurable and the main cause of death. Therefore, exploring the molecular mechanisms of UCB metastasis is of great importance for developing more efficient anticancer treatments. Amplification of chromosome 20q, a region associated with an aggressive tumor phenotype, is one of the most common chromosomal mutations in many neoplasms, including breast, colon, and pancreatic cancers, as well as in UCB.[22] Recently, we profiled 99 UCB tumors for copy number alterations (CNAs) by whole-genome sequencing and revealed that 20q was one of the regions with predominantly recurrent increased DNA sequence copy numbers.[7] This region encodes dominant genes that may

FIGURE 6 ZHX3-induced protumorigenic activity in UCB cells is mediated through RGS2. A, B, Knockdown of RGS2 rescued the invasion and migration capacity of UCB cells with *ZHX3* knockdown in vitro. Error bars show the mean ± SD of 3 independent experiments. **$P < .01$. C, In mouse models, knockdown of RGS2 increased the metastatic ability in T24-shZHX3 cells (6 mice per group). The mean bioluminescent signals are shown in the column. Error bars indicate the mean ± SD. D, Representative lung metastatic nodules (indicated by arrows) and H&E staining of lung tissue are shown (original magnification: ×100; scale bar: 100 μm). Lung tissue was taken from the mice at 6 wk after injection of UCB cells. ns: negative significance. Error bars indicate the mean ± SD. **$P < .01$. E, Knocking down *RGS2* could reverse protein levels of RhoA in T24-shZHX3 cells. F, Knocking down *RGS2* could reversed RhoA activation in T24-shZHX3 cells
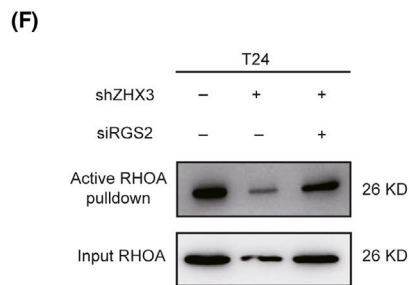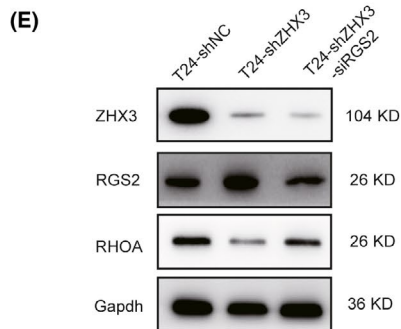
(A)

T24-shNC T24-shZHX3 T24-shZHX3-siRGS2

- T24-shNC
- T24-shZHX3
- T24-shZHX3-siRGS2

The number of invaded cells

(B)

T24-shNC T24-shZHX3 T24-shZHX3-siRGS2

0 h

24 h

- T24-shNC
- T24-shZHX3
- T24-shZHX3-siRGS2

Relative cell migration (%)

(C)

T24-shNC T24-shZHX3 T24-shZHX3-shRGS2

0 week

6 week

Luminescence
1600
1400
1200
1000
800

Color Scale
Min = 667
Max =1627

- T24-shNC
- T24-shZHX3
- T24-shZHX3-shRGS2

Luminescence Intensity (×10⁶ p s⁻¹)

0 Week   6 Week

ns   **   **

(D)

T24-shNC T24-shZHX3 T24-shZHX3-shRGS2

- T24-shNC
- T24-shZHX3
- T24-shZHX3-shRGS2

Number of metastasis nodules in the lungs

(E)

130 KD

T24-shNC T24-shZHX3 T24-shZHX3-siRGS2

ZHX3   104 KD
RGS2   26 KD
RHOA   26 KD
Gapdh   36 KD

(F)

T24

shZHX3   − + +
siRGS2   − − +

Active RHOA pulldown   26 KD
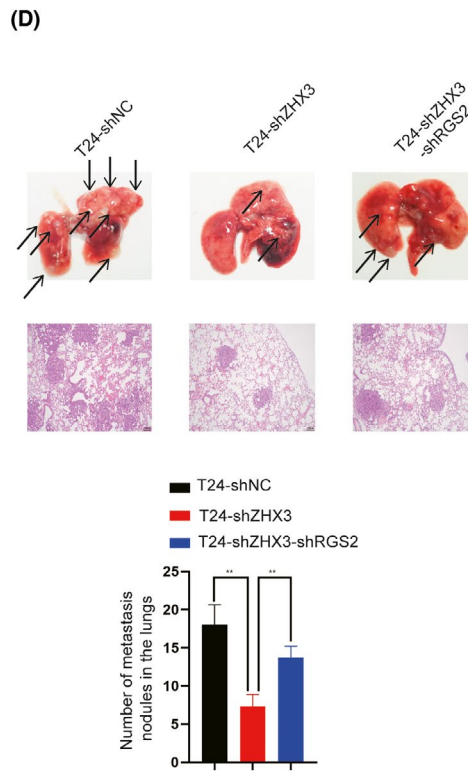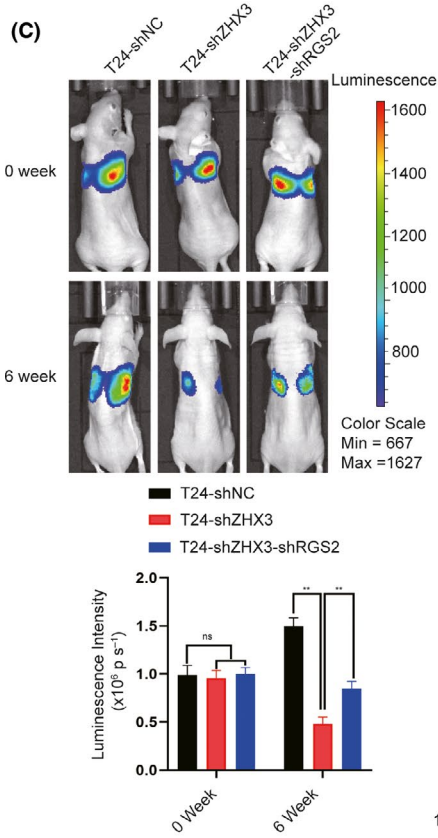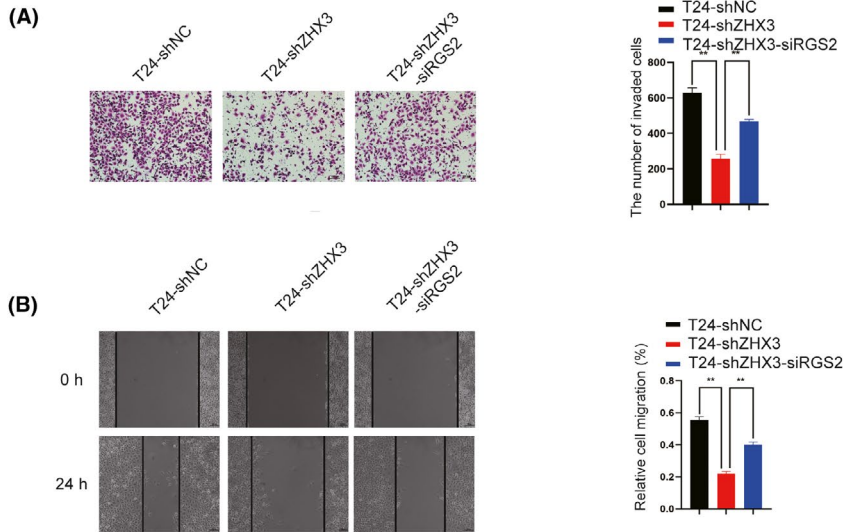Input RHOA   26 KD

FIGURE 7 Low ZHX3 expression combined with high RGS2 expression predicts the best prognosis of patients with UCB. A, High expression of ZHX3 and low expression of RGS2 were examined by IHC in 1 UCB case (top), and low expression of ZHX3 and overexpression of RGS2 were examined by IHC in another UCB case (below). The correlation between the expression levels of ZHX3 and RGS2 was evaluated in 199 UCB tissues, and the results showed that ZHX3 expression levels are negatively correlated with RGS2. *$P < .05$. B, C, Further Kaplan-Meier analysis revealed that patients with both low ZHX3 and high RGS2 expression had the best survival rate in the SYSUCC cohort ($P < .0001$). D, Graphical representation reveals a proposed model for the role and major mechanism of the ZHX3/RGS2/RhoA signaling pathway in regulating the progression of UCB cells
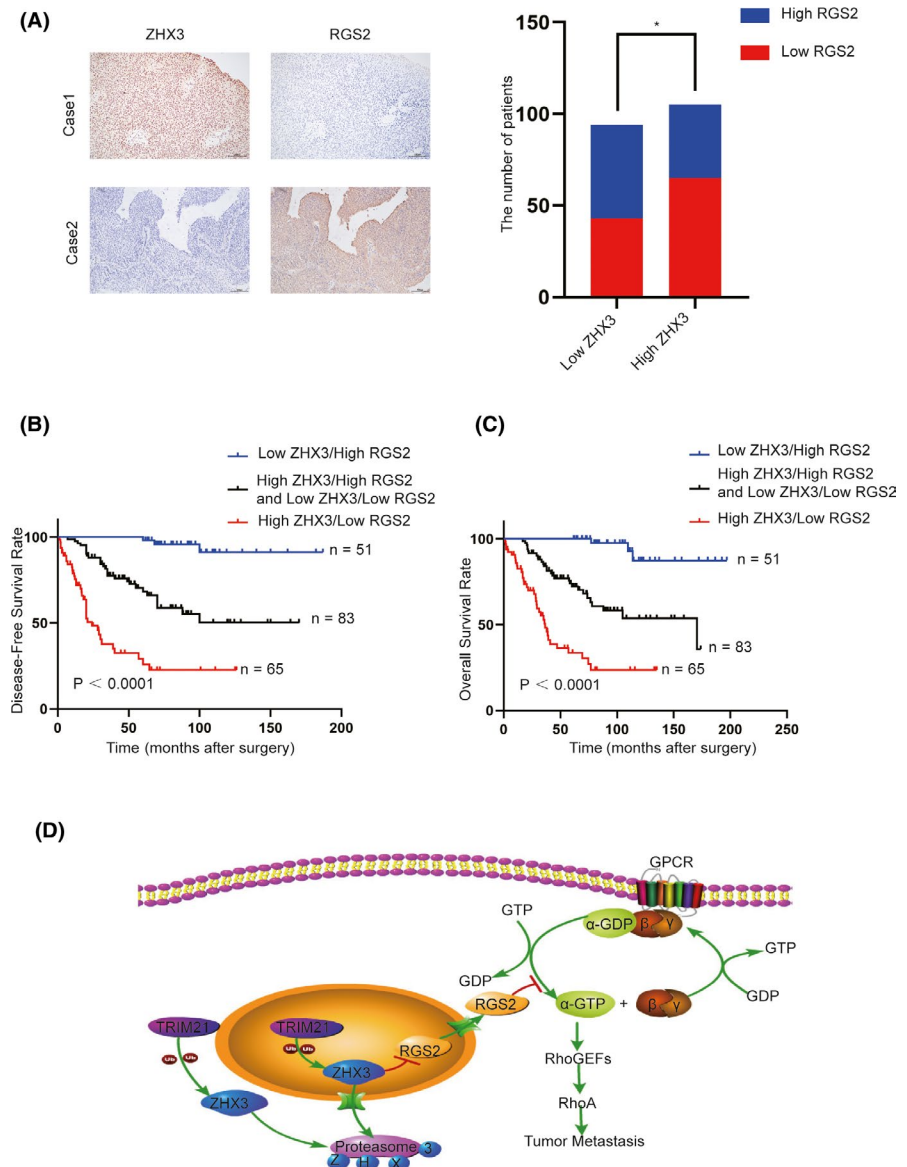
play critical roles in UCB progression and/or serve as therapeutic targets.

In the current study, we characterized a candidate oncogene, *ZHX3*, which is located on 20q12, in the pathogenesis of UCB. We revealed that: (i) ZHX3 DNA sequence copy numbers were frequently increased in UCBs; (ii) ZHX3 was highly expressed in UCB cells and tissue; and (iii) high ZHX3 expression was positively correlated with worse clinical parameters. These data suggested that high expression of ZHX3 plays a crucial role in the development and/or progression of UCB as an oncogenic factor.

As the potential functions of ZHX3 in UCB remain unknown, some experiments were performed in vitro and in vivo in UCB cell lines at our laboratory. Functional studies demonstrated that ZHX3 could enhance UCB cell migration and invasion capacities both in vitro and in vivo. Subsequently, we clarified that ZHX3 acts as a substrate of TRIM21, a protein involved in multiple functions in UCB cells. As a member of the TRIM family, TRIM21 can act as a ubiquitin E3 ligase to degrade different proteins.[23-25] Previous studies have

shown that TRIM21 is involved in cancer development and plays a tumor suppressor role in breast cancer and diffuse large B-cell lymphomas.[26,27] It has been reported that TRIM21 can downregulate the expression of p62 and Nrf2, which act as oncogenes in bladder cancer.[28-30] Our present data showed that ZHX3 is a novel substrate of TRIM21, which then regulates the protein level of ZHX3. Although we cannot confirm whether TRIM21 could inhibit the progression of UCB cells, activation of TRIM21 to degrade ZHX3 protein may still be a promising therapeutic strategy for UCB.

To clarify the downstream target genes and molecular pathways of ZHX3 and UCB metastasis, a Human Tumor Metastasis RT2 Profiler PCR Array containing 84 metastasis-related genes was used to compare the mRNA expression levels in T24 cells with or without knockdown of ZHX3. RGS2 seemed to be a downstream target of ZHX3 in UCB cells and further mechanistic studies showed that RGS2 could be downregulated by ZHX3 through repressing RGS2 mRNA levels.

In our study, we further demonstrated that depleting RGS2 in ZHX3-knockdown UCB cells can effectively rescue the invasion

and migration abilities of these cells both in vitro and in vivo. ZHX3 expression is negatively correlated with RGS2 expression, supporting the important regulatory role of the ZHX3-RGS2 axis in mediating metastasis. RGS2 can accelerate the intrinsic GTPase activity of Gα proteins and interfere with G protein-coupled receptor (GPCR) signaling pathway transduction.[31] In the human genome, RGS2 is considered the most potent negative regulator of $G_q\alpha$ and attenuates $G_q\alpha$-, $G_i\alpha$-, and $G_s\alpha$-mediated pathways.[20] To date, as the most potent negative regulator of $G_q\alpha$, RGS2 has been reported to act as a tumor suppressor in certain human cancers, such as breast, prostate, ovarian, and bladder cancers.[18,32-34] A previous study stated that RGS2 can inhibit the activation of RhoA by negatively regulating heterotrimeric G protein signaling.[35] As a classical oncogene, RhoA is generally considered to be tumorigenic.[36] Similarly, high RhoA expression was closely associated with muscle invasion and metastasis in UCB.[37] In this study, we further identified that ZHX3 could enhance RhoA activity by downregulating RGS2. Taken together, our study results suggested a critical role for ZHX3 in the aggressive progression of UCB through the RGS2/RhoA pathway.

In summary, our present study provides the newest evidence that ZHX3 could be regarded as an oncogenic factor as well as a prognostic biomarker in UCB. Mechanistically, ZHX3 is targeted by TRIM21 to regulate its protein stability and acts as an oncogenic driver in UCB through the RGS2/RhoA pathway (Figure 7D). These data suggest that ZHX3 is a potential therapeutic target for patients with UCB.

ACKNOWLEDGMENTS

DISCLOSURE

The authors have declared that no competing interest exists.

ORCID

Dan Xie https://orcid.org/0000-0003-2242-3138

REFERENCES

1. Ferlay J, Steliarova-Foucher E, Lortet-Tieulent J, et al. Cancer incidence and mortality patterns in Europe: estimates for 40 countries in 2012. *Eur J Cancer*. 2013;49(6):1374-1403.
2. Knowles MA, Hurst CD. Molecular biology of bladder cancer: new insights into pathogenesis and clinical diversity. *Nat Rev Cancer*. 2015;15(1):25-41.
3. Anzick SL. AIB1, a steroid receptor coactivator amplified in breast and ovarian cancer. *Science*. 1997;277(5328):965-968.
4. Collins C, Ferlay J, Steliarova-Foucher E, et al. Positional cloning of ZNF217 and NABC1: genes amplified at 20q13.2 and overexpressed in breast carcinoma. *Proc Natl Acad Sci USA*. 1998;95(15):8703-8708.
5. Sen S, Zhou H, White RA. A putative serine/threonine kinase encoding gene BTAK on chromosome 20q13 is amplified and overexpressed in human breast cancer cell lines. *Oncogene*. 1997;14(18):2195-2200.
6. Tanner MM, Tirkkonen M, Kallioniemi A, et al. Independent amplification and frequent co-amplification of three nonsyntenic regions on the long arm of chromosome 20 in human breast cancer. *Cancer Res*. 1996;56(15):3441-3445.
7. Guo G, Sun X, Chen C, et al. Whole-genome and whole-exome sequencing of bladder cancer identifies frequent alterations in genes involved in sister chromatid cohesion and segregation. *Nat Genet*. 2013;45(12):1459-1463.
8. Suehiro F, Nishimura M, Kawamoto T, et al. Impact of zinc fingers and homeoboxes 3 on the regulation of mesenchymal stem cell osteogenic differentiation. *Stem Cells Dev*. 2011;20(9):1539-1547.
9. Wang L, Liu Q, Kitamoto T, et al. Identification of insulin-responsive transcription factors that regulate glucose production by hepatocytes. *Diabetes*. 2019;68(6):1156-1167.
10. Yamada K, Kawata H, Shou Z, et al. Analysis of zinc-fingers and homeoboxes (ZHX)-1-interacting proteins: molecular cloning and characterization of a member of the ZHX family, ZHX3. *Biochem J*. 2003;373(Pt 1):167-178.
11. You Y, Ma Y, Wang Q, Ye Z, Deng Y, Bai F. Attenuated ZHX3 expression serves as a potential biomarker that predicts poor clinical outcomes in breast cancer patients. *Cancer Manag Res*. 2019;11:1199-1210.
12. Zhang J, Wu T, Simon J, et al. VHL substrate transcription factor ZHX2 as an oncogenic driver in clear cell renal cell carcinoma. *Science*. 2018;361(6399):290-295.
13. Kwon RJ, Han M-E, Kim Y-J, et al. Roles of zinc-fingers and homeoboxes 1 during the proliferation, migration, and invasion of glioblastoma cells. *Tumour Biol*. 2017;39(3):1010428317694575.
14. Paner GP, Stadler WM, Hansel DE, Montironi R, Lin DW, Amin MB. Updates in the eighth edition of the tumor-node-metastasis staging classification for urologic cancers. *Eur Urol*. 2018;73(4):560–569.
15. Xie D, Lau SH, Sham JST, et al. Up-regulated expression of cytoplasmic clusterin in human ovarian carcinoma. *Cancer*. 2005;103(2):277-283.
16. Wei WS, Chen X, Guo L-Y, et al. TRIM65 supports bladder urothelial carcinoma cell aggressiveness by promoting ANXA2 ubiquitination and degradation. *Cancer Lett*. 2018;435:10-22.
17. Wada K, Kamitani T. Autoantigen Ro52 is an E3 ubiquitin ligase. *Biochem Biophys Res Commun*. 2006;339(1):415-421.
18. Liu Y, Ma D, Ji C. Zinc fingers and homeoboxes family in human diseases. *Cancer Gene Ther*. 2015;22(5):223-226.
19. Ying L, Lin J, Qiu F, et al. Epigenetic repression of regulator of G-protein signaling 2 by ubiquitin-like with PHD and ring-finger domain 1 promotes bladder cancer progression. *FEBS J*. 2015;282(1):174-182.
20. Heximer SP, Knutsen RH, Sun X, et al. Hypertension and prolonged vasoconstrictor signaling in RGS2-deficient mice. *J Clin Invest*. 2003;111(4):445-452.
21. Yu OM, Brown JH. G protein-coupled receptor and RhoA-stimulated transcriptional responses: links to inflammation, differentiation, and cell proliferation. *Mol Pharmacol*. 2015;88(1):171-180.
22. Zamostiano R, Pinhasov A, Gelber E, et al. Cloning and characterization of the human activity-dependent neuroprotective protein. *J Biol Chem*. 2001;276(1):708-714.
23. Gallardo-Vara E, Ruiz-Llorente L, Casado-Vela J, Ruiz-Rodríguez MJ. Endoglin protein interactome profiling identifies TRIM21 and galectin-3 as new binding partners. *Cells*. 2019;8(9): 1082.
24. Jin Y, Zhang Y, Li B, et al. TRIM21 mediates ubiquitination of Snail and modulates epithelial to mesenchymal transition in breast cancer cells. *Int J Biol Macromol*. 2019;124:846-853.

25. Clift D, So C, McEwan WA, et al. Acute and rapid degradation of endogenous proteins by Trim-Away. *Nat Protoc*. 2018;13(10):2149-2175.

26. Zhou W, Zhang Y, Zhong C, et al. Decreased expression of TRIM21 indicates unfavorable outcome and promotes cell growth in breast cancer. *Cancer Manag Res*. 2018;10:3687-3696.

27. Brauner S, Zhou W, Backlin C, et al. Reduced expression of TRIM21/Ro52 predicts poor prognosis in diffuse large B-cell lymphoma patients with and without rheumatic disease. *J Intern Med*. 2015;278(3):323-332.

28. Tsai YS, Zhou W, Backlin C, et al. Prothymosin-α enhances phosphatase and tensin homolog expression and binds with tripartite motif-containing protein 21 to regulate Kelch-like ECH-associated protein 1/nuclear factor erythroid 2-related factor 2 signaling in human bladder cancer. *Cancer Sci*. 2019;110(4):1208-1219.

29. Li T, Jiang D, Wu K. p62 promotes bladder cancer cell growth by activating KEAP1/NRF2-dependent antioxidative response. *Cancer Sci*. 2020;111(4):1156-1164.

30. Ciamporcero E, Daga M, Pizzimenti S, et al. Crosstalk between Nrf2 and YAP contributes to maintaining the antioxidant potential and chemoresistance in bladder cancer. *Free Radic Biol Med*. 2018;115:447-457.

31. Kehrl JH, Sinnarajah S. RGS2: a multifunctional regulator of G-protein signaling. *Int J Biochem Cell Biol*. 2002;34(5):432-438.

32. Lyu JH, Park D-W, Huang B, et al. RGS2 suppresses breast cancer cell growth via a MCIP1-dependent pathway. *J Cell Biochem*. 2015;116(2):260-267.

33. Wolff DW, Xie Y, Deng C, et al. Epigenetic repression of regulator of G-protein signaling 2 promotes androgen-independent prostate cancer cell growth. *Int J Cancer*. 2012;130(7):1521-1531.

34. Cacan E. Epigenetic regulation of RGS2 (Regulator of G-protein signaling 2) in chemoresistant ovarian cancer cells. *J Chemother*. 2017;29(3):173-178.

35. Kim Y, Ghil S. Regulators of G-protein signaling, RGS2 and RGS4, inhibit protease-activated receptor 4-mediated signaling by forming a complex with the receptor and Gα in live cells. *Cell Commun Signal*. 2020;18(1):86.

36. Rodrigues P, Macaya I, Bazzocco S, et al. RHOA inactivation enhances Wnt signalling and promotes colorectal cancer. *Nat Commun*. 2014;5:5458.

37. Kamai T, Tsujii T, Arai K, et al. Significant association of Rho/ROCK pathway with invasion and metastasis of bladder cancer. *Clin Cancer Res*. 2003;9(7):2632-2641.

38. Humphrey PA, Moch H, Cubilla AL, Ulbright TM, Reuter VE. The 2016 WHO classification of tumours of the urinary system and male genital organs-Part B: prostate and bladder tumours. *Eur Urol*. 2016;70(1):106–119.

SUPPORTING INFORMATION

Additional supporting information may be found online in the Supporting Information section.